

17 May 1969
MEP

AD 740882

046-830

(N)

THE INTERSTELLAR ABSORPTION IN SELECTED AREA 47

Julian J. Schreier

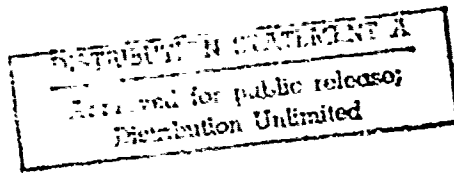
Steward Observatory, University of Arizona, Tucson, Arizona

ABSTRACT

Reproduced by
**NATIONAL TECHNICAL
INFORMATION SERVICE**
Springfield, Va. 22151

A study of the obscuration in the direction of
Selected Area 47 ($l^{II} = 159^{\circ}$, $b^{II} = -21^{\circ}$) has been made.

An absorbing cloud was found at a distance of 300 pc with
a total visual absorption of 2.0 magnitudes.



30

I. INTRODUCTION

There is a great deal of obscuration in the direction of the Per II association. Heeschen (1951) has studied the obscuration in a region of Perseus which includes the association and has found a cloud with a distance of 200 to 300 pc and a total absorption ranging up to and surpassing 2.3 magnitudes.

Selected Area (SA) 47 is located at the southwestern edge of the Per II association and is outside but adjacent to the region studied by Heeschen. Its central star (HD 21483) has been classed by Blaauw (1952) as an association member on the basis of its proper motion. Because this star is more highly reddened than the other association members, and because it shows the strongest λ 4430 interstellar absorption band, an investigation of the obscuration in SA 47 seemed appropriate. This study was accomplished through the use of star counts obtained from photoelectrically-calibrated direct plates.

II. Observational Data

Red and blue plates of both SA 47 and a nearby comparison field were secured at the 84-inch telescope of the Kitt Peak National Observatory by Dr. B. J. Bok. The comparison field is centered on the star BD +31° 588, and is located about 2.5 degrees to the northwest of SA 47. These plates have useful fields of about 0.25 square degrees. Table I gives the data of the plates.

In order to calibrate the plates, photoelectric sequences were established in each field. The UBV observations were obtained on four nights with the Steward Observatory 36-inch telescope. The B and V magnitudes and, where available, the U-B color are listed in Table II.

Red magnitudes (R) were calculated from the UBV photometry by the formula, after Becker (1965),

$$V-R = 0.32 + 0.22 (B-V) + 0.04 (U-B).$$

Because no U magnitudes were obtained for the faintest stars, the formula

$$V-R = 0.32 + 0.26 (B-V)$$

was used to compute their red magnitudes. The use of the latter formula introduces only small errors into the computed magnitudes, on the order of two or three hundredths of a magnitude. The R magnitudes computed from each night's UBV photometry are listed in Table III.

III. The Reductions

The plates were measured on the Cuffey iris photometer of the Steward Observatory. The iris readings of the photoelectric standards were plotted against the observed magnitudes, and calibration curves were drawn through the points (Figures 1 and 2). For both plates of the comparison field the calibration curves were extrapolated linearly to about 0.5 magnitudes beyond the faintest photoelectric standards. Because the calibration curves for the comparably-exposed plates of SA 4" are linear in this region this extrapolation should be valid.

The iris readings for each plate were converted to magnitudes by means of a linear interpolation from a tabulation of the calibration

curves. To these magnitudes were added the field corrections for the 84-inch telescope. These field corrections have been estimated by Dr. A. A. Hagg (Private communication) from measurements of the areas of extra focal stellar images and arise from optical blocking by the tertiary mirror of the coude system.

IV. The Star Counts

Counts of stars were made for each integral apparent magnitude over the interval from $m-\frac{1}{2}$ to $m+\frac{1}{2}$. The counts were then analyzed by means of Wolf diagrams (Wolf 1923), and through the use of $(m, \log W)$ tables (Bok 1937).

Both the $(m, \log W)$ method and the Wolf method make the assumption either that there is no obscuration in the comparison field, or that the amount of obscuration is known. From the UBV colors of BD +31° 588, and from the work of Heeschen (1951), it appears that the comparison field has about 0.5 magnitude of obscuration within a distance of a few hundred parsecs. This obscuration would also be present in SA 47, in addition to that which is found by Wolf or $(m, \log W)$ method.

Many stars in a wide region around the Per II association show at least 0.5 magnitude absorption (A. E. Rydgren, private communication). Some of these reddened stars are found as close as 100 pc to the sun. This makes it reasonable to assume that the 0.5 magnitude of obscuration arises from a foreground cloud which need not be part of the heavy concentration seen in SA 47.

The Wolf diagrams (Figures 3 and 4) show an absorption in the blue of two magnitudes, and in the red of slightly less than two magnitudes. The values $A_B = 2.00 \pm 0.15$ magnitudes and $A_R = 1.90 \pm 0.15$ magnitudes are adopted. The Wolf diagrams however yield no information about the distance to the obscuring matter.

The (m , $\log \pi$) analysis was accomplished in the following manner. First the foreground absorption of 0.5 magnitude was adopted, and then a standard table was constructed for the comparison field. To do this a luminosity function had to be assumed.

Up to a distance of 500 pc ($z = -180$ pc, $\log d = 2.7$) a luminosity function appropriate to the galactic plane was used. For the region extending from $d = 500$ pc to $d = 800$ pc a linear combination of the luminosity functions for the galactic plane and for $z = 500$ pc was used. Beyond $d = 800$ pc ($z = -290$ pc, $\log d = 2.9$) the luminosity function for $z = 500$ pc was adopted.

The blue luminosity function adopted for the galactic plane is a combination of the luminosity functions of van Rhijn (1936), and Luyten (1939), as used by Bok and MacRae (1941). The red luminosity function for the galactic plane was constructed from the visual van Rhijn-Luyten luminosity function as follows.

All stars fainter than $M_V = 3$ were assumed to be main-sequence stars. The V-R colors for stars with approximately integral values of M_V along the main sequence were taken from the table of infrared measurements published by Johnson (1966). The V-R colors were then

subtracted from the absolute visual magnitudes to yield absolute red magnitudes for the stars at each point along the main sequence. Clearly the space density of any homogeneous group of stars does not depend on whether we consider the absolute visual or red luminosity for the members of the group. Therefore the space density for main-sequence stars with a given value of M_V is the same as the space density for main-sequence stars with the corresponding value of M_R . This means that by adjusting the absolute luminosities at each point along the visual luminosity function by an amount equal to the appropriate V-R color a red luminosity function may be constructed.

For stars brighter than $M_V = 3$, where stars of a range of spectral types contribute to the number density at a given absolute magnitude, an average B-V color at a given value of M_V was found from a comparison of the blue and visual luminosity functions of van Rhijn. The V-R color was assumed to be equal to the B-V color, and the values of M_V were adjusted by the amount of the corresponding V-R colors to give absolute red magnitudes, which together with the space densities formed the bright end of the red luminosity function. Because of the very low number densities involved, the entries in the $(\pi, \log \pi)$ tables proved to be quite insensitive to errors in adjusting the bright end of the luminosity function. Even an assumption of zero space density for these stars would have changed the predicted star counts by about two stars per unit apparent magnitude interval.

The luminosity functions for $z = 500$ pc were based on the visual

luminosity function for that z distance as determined by Upgren (1963).

Again the stars fainter than $M_V = 3$ were assumed to be on the main sequence, and the B-V and V-R colors were used to adjust the faint end of Upgren's visual luminosity function to form the faint portions of the blue and red luminosity functions.

At $z = 500$ pc, as in the galactic plane, stars with a mixture of spectral types contribute to the bright end of the luminosity function. For the older population encountered at a distance of several hundred parsecs from the galactic plane (Upgren 1963) the absolute magnitude interval from $M_V = +2$ to $M_V = -1$ is represented by the subgiants, red giants and the horizontal branch stars. Therefore at any given M_V in this range one is likely to encounter both blue and red stars. In addition, and for the reasons given previously, the final result is quite insensitive to the adjustment of the bright end of the luminosity function. With these arguments in mind the colors of the GO dwarf ($B-V = 0.6$, $V-R = 0.5$) were used as average colors for the entire range, and the bright portions of the blue and red luminosity functions were formed.

The $(m, \log w)$ tables for the comparison field were then constructed from the derived luminosity functions. As distances greater than 500 pc from the galactic plane were reached the decrease in space density as found by Becker (1965) was allowed for. It was found that only minor adjustments in the space densities and the derived luminosity functions were necessary to bring both the red and blue star counts predicted by the $(m, \log w)$ tables into agreement with the actual star counts.

The (m , $\log \pi$) tables of SA 47 were constructed from the (m , $\log \pi$) tables of the comparison field by adding the effect of various amounts and distances of absorbing material until the predicted star counts were in agreement with the actual star counts.

The final (m , $\log \pi$) tables are shown in Tables IV through X. An examination of these tables will show that A_B probably lies between 2.0 and 2.2 magnitudes, while A_R probably lies between 1.8 and 2.0 magnitudes. This would indicate a total visual absorption of 2.0 magnitudes. It is particularly interesting to note that even when a very large amount of obscuration is assumed at a distance of 500 pc many more bright stars are predicted than are actually observed. Thus it appears that 500 pc can be taken as an upper limit for the distance to the obscuring cloud. Because of the low number of nearby stars it was not possible to fix a minimum distance to the cloud.

V. The Star HD 21483

The Per II association member HD 21483 has a color excess, $E(R-V)$, of 0.55 magnitude, which under the assumption that $A_V/E(B-V) = 3.0$ would mean that $A_V = 1.65$ magnitudes. This star has a radial velocity of -6 km/sec while the mean for the association is nearly +20 km/sec (Blaauw 1962). Since the expansion age of the association is 1.3×10^6 years (Blaauw 1962), association membership would place the star some 30 pc closer than the association, or at a distance of

300 pc. Under the above assumption of the ratio of total to selective absorption this is just the distance the star would be at if it were a B3 dwarf.

Morgan, however, has classified HD 21483 as type B3 III (Morgan, Code, and Whitford 1955). Also Lesh (1968) has used it as a fundamental standard for class B3 III, and lists criteria for the classification. If the star is indeed a giant it should be located well behind the association and moving rapidly toward it, a circumstance which would make association membership unlikely, and the star's proper motion away from the center of the association fortuitous.

Another possibility does exist. If the ratio of total to selective absorption were anomalously high, say 5 or 6 as has been found for some B stars, then HD 21483 could be a giant and still be at a distance of 300 pc. Such a possibility would seem to be indicated by the small difference in the total absorption in the blue and red which was found for the obscuring cloud. Infrared photometry of HD 21483 should be able to resolve this question.

VI. Summary

An obscuring screen in front of Selected Area 47 was found to have a total absorption in the blue of 2.10 ± 0.15 magnitudes. The absorption in the red was found to be 1.90 ± 0.15 magnitudes, which makes a visual absorption of 2.00 ± 0.15 magnitudes seem reasonable. There probably is an additional 0.5 magnitude foreground obscuration in this area.

The distance to the 2.0 magnitude obscuring screen is placed at 300 ± 200 pc. It seems likely that it is part of the larger cloud found by Heeschen, in spite of its apparent compactness. It is possible that the dust is connected with the Per II association.

Acknowledgments

The author wishes to thank Dr. B. T. Lynds who suggested this topic, and under whose direction this work was carried out. Dr. Lynds proved to be the source of frequent helpful suggestions and much assistance during the course of this study.

Thanks go also to Dr. B. J. Bok for securing the plates used in the study, and to Dr. B. E. Westerlund and Dr. R. E. White for their assistance in the preparation of this paper.

The data reductions were carried out on the CDC 6400 computer of the Numerical Analysis Laboratory of the University of Arizona. This work was supported by the Office of Naval Research under grant number N00014-67-C-0322.

References

- Becker, W., 1965, Z. Astrophys., 62, 59.
- Blaauw, A., 1952, B.A.N., 11, 405.
- Bok, B. J., 1937, The Distribution of the Stars in Space,
(Chicago. University of Chicago Press)
- Bok, B. J., and MacRae, D. C., 1941, Ann. N.Y. Acad. Sci., 42, 219.
- Heeschen, D. S., 1951, Astrophys. J., 114, 132.
- Johnson, H. L., 1966, Ann. Rev. of Astron and Astrophys., 4, 193.
- Lesh, J., 1968, Astrophys. J. Supp., 17, 371.
- Luyten, W. J., 1939, Minn. Publ., 2, No. 7.
- Morgan, W. W., Code, A. D., and Whitford, A. E., 1955, Astrophys. J. Supp.,
2, 41.
- Upgren, A. R. Jr., 1963, Astron. J., 68, 475.
- van Rhijn, P. J., 1936, Gron. Publ., No. 47.
- Wolf, M., 1923, Astron. Nachr., 219, 109.

Captions for Figures

- Figure 1.** Photoelectric magnitude vs. iris reading for the sequence stars in SA 47. The open circles represent red magnitudes and the crosses represent blue magnitudes.
- Figure 2.** Photoelectric magnitude vs. iris reading for the sequence stars in the comparison field. The open circles represent red magnitudes and the crosses represent blue magnitudes.
- Figure 3.** Star counts in blue light (after Wolf 1923). The crosses refer to SA 47 and the open circles refer to the comparison field. The broken line represents the expected star count for a uniform distribution of stars. The ordinate is $\log N(m_B)$, the number of stars brighter than magnitude m_B .
- Figure 4.** Star counts in red light (after Wolf 1923). The crosses refer to SA 47 and the open circles refer to the comparison field. The broken line represents the expected count for a uniform distribution of stars. The ordinate is $\log N(m_R)$, the number of stars brighter than magnitude m_R .
- Figure 5.** The observed visual luminosity functions. The solid line is the Van Rhijn/Luyten luminosity function for the galactic plane and the broken line is Upgren's visual luminosity function for $z=500$ pc.
- Figure 6.** The adopted blue luminosity functions. The solid line represents the stellar distribution in the galactic plane and the broken line represents the distribution of stars at a distance ~ 500 pc from the galactic plane.
- Figure 7.** The adopted red luminosity functions. The solid line represents the stellar distribution in the galactic plane and the broken line represents the distribution of stars at a distance of 500 pc from the galactic plane.

TABLE I. Plate data

PLATE	DATE	EMULSION/FILTER	EXPOSURE	R. A.	DEC.	FIELD
686	11/06/66	103a0 + GG 13	60 min.	3 ^h 26.5 ^m	+30°.2	SA 47
706	11/10/66	103aE + RG 1	30 min.	3 ^h 26.5 ^m	+30°.2	SA 47
707	11/10/66	103a0 + GG 13	30 min.	3 ^h 20.3 ^m	+32°.1	Comp.
708	11/10/66	103aE + RG 1	60 min.	3 ^h 20.3 ^m	+32°.1	Comp.

TABLE II. Photoelectric data for SA 47

STAR	COLOR					ADOPTED B MAGNITUDE
		1/21/68	9/20/68	9/22/68	11/23/68	
1	V	7.07				
	B	7.40				7.40
	U-B	-0.32				
2	V		9.90	9.83		
	B		10.42	10.39		10.41
	U-B		-0.05	-0.04		
3	V	10.26	10.25			
	B	10.93	10.93			10.93
	U-B	0.26	0.36			
4	V		11.09	11.06		
	B		11.73	11.69		11.71
	U-B		0.09	0.09		
5	V		12.07	11.99		
	B		12.74	12.65		12.69
	U-B		0.31	0.05		
6	V	12.96	12.99			
	B	14.34	14.40			14.37
	U-B	1.11	1.50			
7	V	14.09	14.28		14.03	
	B	15.31	15.31		15.31	15.31
	U-B	0.83	—		0.88	
8	V	14.69	14.63			
	B	15.91	15.92			15.92
	U-B	0.55	0.68			
9	V	14.72	14.74	14.90	14.65	
	B	16.03	16.04	16.15	15.97	16.05
	U-B	0.67	1.48	—	0.63	
10	V	15.09	14.86		14.63	
	B	15.92	15.74		15.75	15.80
	U-B	0.49	—		0.25	
11	V	15.63		15.58		
	B	16.66		16.75		16.71
	U-B	0.82		0.58		
12	V				16.87	
	B				17.74	17.74
	U-B				—	
13	V	16.62		16.87	16.67	
	B	17.44		18.35	17.75	17.85
	U-B	—		—	—	
14	V	16.96		17.03		
	B	17.86		18.47		18.16

TABLE IIb. (Photoelectric Data for the Comparison Field)

STAR	COLOR	DATE				ADOPTED B MAGNITUDE
		1/21/68	9/20/68	9/22/68	11/23/68	
1	V	7.43		7.52	7.33	
	B	9.31		9.39	9.26	9.32
	U-B	2.09		1.90	2.17	
2	V	10.78		10.81		
	B	12.25		12.28		12.26
	U-B	1.48		1.52		
3	V	11.94		11.91		
	B	13.32		13.36		13.34
	U-B	1.23		1.30		
4	V				12.04	
	B				13.27	13.29
	U-B				0.87	
5	V	12.33		12.35		
	B	13.63		13.65		13.64
	U-B	1.12		1.20		
6	V		12.55	12.49		
	B		14.04	13.96		14.00
	U-B		1.39	1.43		
7	V			12.58		
	B			13.43		13.43
	U-B			0.33		
8	V		13.38	13.38		
	B		14.12	14.09		14.10
	U-B		0.10	0.25		
9	V			14.91		
	B			15.97		15.97
	U-B			0.6		
10	V			14.45		
	B			15.80		15.80
	U-B			0.41		
11	V			15.01		
	B			15.71		15.71
	U-B			0.08		
12	V			15.69		
	B			17.22		17.22
	U-B					

TABLE III. Red Magnitudes Computed From UBV Photometry

STAR	DATE				ADOPTED R MAGNITUDE
	1/21/68	9/20/68	9/22/68	11/23/68	
(SA 47)					
1	6.71				6.71
2		9.47		9.39	9.43
3	9.79	9.76			9.77
4			10.62	10.60	10.61
5			11.59	11.53	11.56
6	12.29	12.30			12.29
7	13.47	13.71		13.46	13.52
8	14.08	14.22			14.17
9	14.08	14.07	14.24	14.01	14.11
10	14.57	14.33		14.30	14.36
11	15.05		15.10		15.08
12				16.32	16.32
13	16.08		16.18	16.10	16.12
14	16.40		16.34		16.37
(Comparison Field)					
1	6.62		6.71	6.50	6.61
2	10.07		10.11		10.09
3	11.27		11.21		11.24
4			11.46	11.41	11.44
5	11.68		11.69		11.65
6			11.86	11.79	11.83
7				12.06	12.06
8		12.90		12.87	12.88
9				13.23	13.93
10				14.43	14.43
11				14.51	14.51
12				15.04	15.04

Table IV. The (m , $\log \pi$) table in blue light for the comparison field.

$\log \pi$	6	7	8	9	10	11	12	13	14	15	16	17	18	19
-1.6														
-1.8														
-2.0		0.1	0.1	0.1	0.1	0.1	0.1	0.1	0.1	0.1	0.1	0.1	0.1	0.1
-2.2	0.1	0.1	0.2	0.2	0.3	0.4	0.5	0.5	0.6	0.6	0.8	0.9	1.1	1.3
-2.4	0.1	0.2	0.4	0.8	1.0	1.3	1.7	2.0	2.4	2.4	3.0	3.7	4.3	
-2.6	0.2	1.0	1.5	3.0	3.9	5.1	6.7	8.1	9.7	12.0	14.6			
-2.8	0.2	0.2	0.2	0.2	2.2	5.5	6.0	26.6	36.6	40.0	47.0			
-3.0	0.1	0.3	0.4	0.3	2.2	4.0	10.0	36.6	109.8	153.7				
-3.2		0.1	0.4	0.5	0.4	2.6	6.6	12.0	43.8	131.4				
-3.4			0.1	0.5	0.7	0.5	3.5	8.7	18.0	58.1				
-3.6					0.1	0.6	0.8	0.6	4.2	10.4	18.0			
-3.8						0.2	0.8	1.1	0.8	5.5	13.8			

Number of stars predicted	0.2	0.5	2.0	3.2	5.5	9.3	17.1	24.3	60.0					
Number of stars counted	1	1	1	1	5	7	16	21	60					

Table V. The $(m, \log \pi)$ table in red light for the comparison field.

$\log \pi$	5	6	7	8	9	10	11	12	13	14	15	16	17	18	19
-1.6															
-1.8															
-2.0															
-2.2															
-2.4															
-2.6															
-2.8															
-3.0															
-3.2															
-3.4															
-3.6															
-3.8															

Number of stars predicted	0.3	0.6	1.9	3.3	6.4	10.5	21.3	70.0	127.8
Number of stars counted	1	1	2	9	13	23	71	128	128

Table VI. The (m , $\log \pi$) table in blue light for SA 47,
assuming an absorption of 2.2 magnitudes at a distance of 300 pc.

$\log \pi$	6	7	8	9	10	11	12	13	14	15	16	17	18	19
-1.6														
-1.8														
-2.0					0.1	0.1	0.1	0.1	0.2	0.2	0.2	0.2	0.3	0.4
-2.2				0.1	0.1	0.2	0.2	0.3	0.4	0.5	0.6	0.8	0.9	1.1
-2.4				0.1	0.2	0.4	0.8	1.0	1.3	1.7	2.0	2.4	3.0	3.7
-2.6				0.1	0.2	0.4	0.8	1.0	1.4	2.7	3.7	4.9	6.4	7.8
-2.8						0.2	0.8	1.4	2.7	3.7	4.9	6.4	7.8	9.4
-3.0						0.1	0.3	0.4	0.3	0.3	1.8	3.6	8.8	31.3
-3.2							0.1	0.3	0.5	0.4	0.4	2.2	5.8	10.9
-3.4								0.1	0.4	0.7	0.5	2.9	7.7	
-3.6									0.1	0.5	0.8	0.6	3.5	
-3.8										0.2	0.7	1.0	0.9	

Number of stars predicted	0.2	0.3	0.7	1.3	2.5	3.8	6.1	9.7	17.0	24.4	54.6
Number of stars counted	1	2	1	1	5	4	17	25	50		

Table VII. The ($m, \log \Pi$) table in blue light for SA 47,
assuming an absorption of 2.0 magnitudes at a distance of 300 pc.

$\log \Pi$	6	7	8	9	10	11	12	13	14	15	16	17	18	19
-1.6														
-1.8										0.1	0.1	0.1	0.1	0.1
-2.0	0.1	0.1	0.1	0.1	0.1	0.1	0.2	0.2	0.2	0.2	0.2	0.3	0.3	0.4
-2.2	0.1	0.1	0.2	0.2	0.3	0.4	0.5	0.6	0.6	0.8	0.9	1.1	1.1	1.3
-2.4	0.1	0.2	0.4	0.8	1.0	1.3	1.7	2.0	2.4	2.4	3.0	3.7	4.3	
-2.6				0.2	1.0	1.5	3.0	3.9	5.1	6.7	8.1	9.7		
-2.8					0.2	0.2	0.2	2.2	5.5	5.5	6.0	26.6	36.6	
-3.0					0.1	0.3	0.4	0.3	2.2	4.0	10.0	36.6		
-3.2						0.1	0.4	0.5	0.4	0.4	2.6	6.6	12.0	
-3.4							0.1	0.5	0.7	0.5	0.5	3.5	8.7	
-3.6								0.1	0.6	0.8	0.6	0.6	4.2	
-3.8									0.2	0.8	1.1	0.8		

Number of stars predicted	0.2	0.3	0.7	1.3	2.7	3.9	6.5	10.4	18.2	25.7	61.7			
Number of stars counted	1	2	1	1	5	4	17	25	50					

Table VIII. The (m , $\log \pi$) table in blue light for SA 47 which

results from the assumption of a very high ($A_B > 10$) absorption at a distance of 500 pc.

$\log \pi$	6	7	8	9	10	11	12	13	14	15	16	17	18	19
-1.6														
-1.8														
-2.0					0.1	0.1	0.1	0.1	0.1	0.1	0.1	0.1	0.1	0.1
-2.2			0.1	0.1	0.2	0.2	0.3	0.4	0.4	0.5	0.5	0.6	0.8	0.9
-2.4		0.1	0.2	0.4	0.8	1.0	1.3	1.7	2.0	2.4	3.0			
-2.6		0.2	1.0	1.5	3.0	3.9	5.1	6.7	8.1	9.7				
-2.8														
-3.0														
-3.2														
-3.4														
-3.6														
-3.8														

Number of stars predicted	0.2	0.5	1.7	2.6	4.4	5.7	7.5	9.6	11.6
Number of stars counted	1	1	2	1	1	5	4	17	

Table IX. The (m , $\log \pi$) table in red light for SA 47,
assuming an absorption of 1.8 magnitudes at a distance of 300 pc.

$\log \pi$	6	7	8	9	10	11	12	13	14	15	16	17	18	19
-1.6														
-1.8														
-2.0				0.1	0.1	0.1	0.2	0.2	0.2	0.3	0.3	0.3		
-2.2			0.1	0.1	0.1	0.3	0.4	0.5	0.5	0.7	0.8	1.0	1.2	
-2.4		0.1	0.2	0.3	0.6	1.2	1.6	2.1	2.1	2.7	3.3	4.1		
-2.6		0.1	0.3	1.0	1.0	1.5	2.8	4.9	4.9	6.6	8.8			
-2.8		0.2	0.4	0.6	0.6	1.3	3.0	13.1	13.1	29.9				
-3.0			0.2	0.4	0.5	0.5	0.9	5.6	5.6	31.3				
-3.2				0.3	0.5	0.5	0.5	0.5	0.5	0.5	5.1			
-3.4					0.3	0.6	0.6	0.6	0.6	0.6	0.6			
-3.6						0.4	0.6	0.8						
-3.8							0.5	1.0						

Number of stars predicted	0.2	0.3	0.6	1.5	3.3	5.2	8.5	13.9	32.4	83.2				
Number of stars counted	1	1	1	1	5	4	17	27	73					

Table X. The $(m, \log \pi^*)$ table in red light for SA 47, assuming
an absorption of 2.0 magnitudes at a distance of 300 pc.

$\log \pi^*$	6	7	8	9	10	11	12	13	14	15	16	17	18	19
m														
-1.6														
-1.8														
-2.0														
-2.2														
-2.4														
-2.6														
-2.8														
-3.0														
-3.2														
-3.4														
-3.6														
-3.8														

Number of stars predicted	0.2	0.3	0.6	1.3	3.1	4.7	7.8	12.0	22.9	71.8				
Number of stars counted	1		1	1	1	5	4	17	27	73				

